International Journal of Progressive Sciences and Technologies (IJPSAT)
ISSN: 2509-0119.

Vol. 43 No. 2 March 2024, pp. 42-56

Assessment Of Rainfall Disaster Risk In Theaautonomous District Of Abidjan, Côte d'Ivoire

Kinakpefan Michel TRAORE

Department of Geography
Jean Lorougnon Guédé University
Daloa, Côte d'Ivoire
traoremichel50@yahoo.fr

***Abstract*—. In the context of global change and climatic uncertainties, this study addresses the issue of the recurrence of rainfall events which, year after year, are responsible for the loss of many lives and significant material damage in the Autonomous District of Abidjan (ADA). The aim is to use spatial modelling to identify the areas of the district most vulnerable to hydroclimatic events such as flooding, soil erosion and landslides. The method integrates flooding, erodibility and soil loss indices into a Geographic Information System. These indices were generated on the basis of several criteria: soil, slope, lithology, exposure, slope shape and curvature, moisture index, vegetation index, land use and occupation, climatic aggressiveness, soil erodibility, topographic factor and soil protection. They were then prioritised, weighted and aggregated using a multi-criteria approach, the Analytical Hierarchy Process. This approach shows that the hydroclimatic risk associated with extreme weather events, but also and above all with poor territorial development, remains a major risk in the ADA. The analysis shows that almost a third (31.5%) of the territory is vulnerable to extreme hydro-meteorological events, ranging from "very likely" to "certain". This high level of vulnerability affects around two out of five inhabitants of the district. This map remains a decision-making tool for the preventive management of rainfall risk, which is likely to be exacerbated by the effects of climate variability.**

Keywords— Autonomous District of Abidjan, Rainfall risk, Vulnerabilities, Climate disaster, Decision-making tool, Crisis management

I. INTRODUCTION

Every year, the Autonomous District of Abidjan (ADA) experiences increasingly catastrophic extreme rainfall events. This increase in rainfall risk raises the question of the vulnerability of the area to rainfall hazards. Official statistics show that, since the mid-1990s, hydrometeorological events have caused almost 300 deaths or disappearances and significant material damage amounting to several million US dollars (Hauhouot, 2008; GCI, 2019; INS, 2008; Ado and Rey, 2020, POGCI, 2023). Extreme rainfall is indeed a major risk, causing an average of 13 deaths per year in the Abidjan district since 2009 (UNOCHA, 2014; GCI, 2019: 34). In 2022, a total of 11,478 individuals, approximately 1,913 households and lifeline (water, electricity, health, food, roads, sanitation…) was affected by rainfall disasters (IFRC, 2023: 2).

In this post-industrial context, which is peremptorily leading the planet into a new geological era known as the Anthropocene (Wallenhorst et al., 2019: 24), the event that triggers the majority of these hydrometeorological disasters is inevitably the disruption of the elements of climate (Mcbean and Ajibade, 2009; Quenault, 2013: 4). It is clear that climate change is leading to an increase in the frequency and intensity of extreme weather events (Camirand and Gingras, 2011; IPCC, 2014; Salack et al, 2016; Koungbanane et al, 2023: 2). The "novelty" of climate change lies mainly in the intensification of climatic hazards and their occurrence, which global models estimate to be "very likely" (IPCC, 2007).

These extreme events, especially those of an exceptional nature, are predicted to become more frequent (IPCC, 2022). More

Corresponding Author: Kinakpefan Michel TRAORE

than 8 out of 10 natural disasters worldwide are now attributed to climate change and extreme weather events (IFRC, 2020: 19). These climate-related disasters have incalculable impacts in terms of damage, harm and economic, non-economic and environmental losses (IPCC, 2022: 8; Koungbanane et al, 2023: 7). Moreover, these impacts are more significant in cities, especially in the Global South, due to the concentration of people and problems, but also due to the vulnerabilities associated with rapid and disorderly urbanisation (Dpngo et al, 2008: 2; Colombert and Boudes, 2012; p. 3; Traoré, 2023: 262). Disasters, understood as "serious disturbances that affect a community and exceed its capacity to cope" (IFRC, 2020: 3), are a major brake on development (Jah. et al., 2012: 13) and even threaten the sustainability of human settlements (Bertrand, 2010; Quenault, 2013: 4).

Disaster Risk Management (DRM) is seen more as a condition for the existence and continued operation and development of urban areas. However, the DRM dependent on the capacity and effectiveness of local governance and decision-making processes (IPCC, 2022: 20). The failure of local governance raises the question of the resilience of cities to climate change.

This article is therefore part of a global and local effort to reduce vulnerability to extreme precipitation disasters. the aim is to rank the vulnerability to rainfall risk in order to identify the ADA sub-regions that are most vulnerable to this hydrometeorological risk.

This template, modified in MS Word 2007 and saved as a "Word 97-2003 Document" for the PC, provides authors with most of the formatting specifications needed for preparing electronic versions of their papers. All standard paper components have been specified for three reasons: (1) ease of use when formatting individual papers, (2) automatic compliance to electronic requirements that facilitate the concurrent or later production of electronic products, and (3) conformity of style throughout a conference proceedings. Margins, column widths, line spacing, and type styles are built-in; examples of the type styles are provided throughout this document and are identified in italic type, within parentheses, following the example. Some components, such as multi-leveled equations, graphics, and tables are not prescribed, although the various table text styles are provided. The formatter will need to create these components, incorporating the applicable criteria that follow.

II. Materials and Methods

2.1. Study area

The ADA is located on the Ivorian coast between 5°10′0″ and 5°40′0″ north latitude and 4°30′0″ and 4°60′0″ west longitude (Fig. 1). In addition to the city of Abidjan, this territory includes four sub-prefectures: Songon, Anyama, Brofodoumé and Bingerville (Fig. 1).

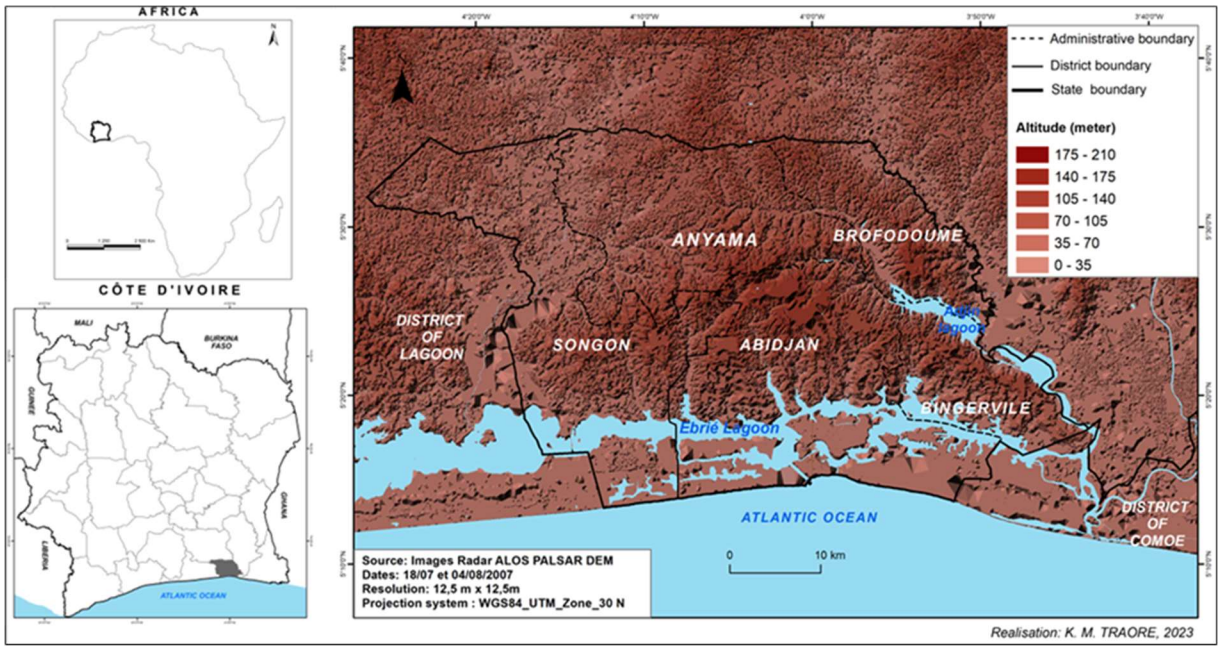

Fig. 1. Location of study area

The morphology of the site is marked by the major tectonic fault of the Ebrié lagoon system which divides the site into two areas: the southern area, consisting of coastal plains with altitudes of less than 20 m, and the northern area, consisting of inland plateaux up to 210 m (BNEDT, 2008; Martin, 1969: 19). The territory of the district is divided into very gentle slopes (≤2%), which are sensitive to water accumulation, and steep slopes (>7%), which are more prone to material movement, covering 44% and 36% of the area respectively (Traoré, 2022: 129).

The dominant geological formations are plateaus, largely composed of more or less ferruginous sandstones, clay sediments, shales and grauwackes (Martin, 1973; BNEDT, 2008: 122). The overlying soils are essentially ferralitic, hydromorphic, podzolic and only slightly developed on marine sands (Roose et al, 1966: 70; BNEDT, 2008: 122).

The coastline on which ADA is located is the wettest region in Côte d'Ivoire, with average annual rainfall of well over 1,500 millimetres (Brou, 2008: 25; Hauhouot, 2008: 77). Rainfall is not only abundant but also continuous, lasting from a few hours to several days (Hauhouot, 2008: 78). The ADA covers an area of 2034 km² and has a population of over 6.3 million.

2.2. Study data

The methodological approach that led to the spatial model for assessing vulnerability to rainfall risk mobilised a certain amount of geospatial data (Table 1). This includes topographical, pedological, lithological, climatological and soil protection data.

TABLE I. STUDY DATA

N°	Type	Sources	Resolution	Date
1	Topographical	https://search.asf.alaska.edu/#/	12,5 m	18/07/2007
2	Pedological	https://www.fao.org/soils-portal/fr/	0.5° x 0.5°	January 2003
3	Lithological	ORSTROM, Côte d'Ivoire	-	1972
4	Climatological	crudata.uea.ac.uk/cru/data/hrg / SODEXAM	0.5° x 0.5°	1971-2020
5	Land Use	https://scihub.copernicus.eu/	10 m	01/01 -31/12/22

Source : https://asf.alaska.edu; https://scihub.copernicus.eu/, https://www.fao.org/soils-portal/fr/

2.3. Methods

The method involved processing the climate data and mapping the levels of rainfall risk in the ADA.

Climate data processing

Climatic data were processed to determine the variability of climatic parameters, in particular temperature and precipitation. The intensity of precipitation was also determined using a climatic aggressiveness index (R factor).

Variability of climate parameters

The aim was to detect breaks and calculate rainfall indices to understand the variability of rainfall. There are several tests to detect breaks (BUISHAN test and BOIS ellipse, LEE and HEGHINAN Bayesian method, Hubert segmentation, etc.). In this study, we used the Pettitt (1979) test. This is a non-parametric test derived from the Mann and Whitney (1947) test (Adou et al, 2020: 14). The test assumes that there is no break in the rainfall time series (Xi) of size N. This assumption is the null hypothesis and the presence of a break is the alternative hypothesis. The implementation of the test assumes that for t between 1 and N, the time series (Xi), i=1 to t and t+1 to N belong to the same population.

The variable to be tested is the maximum of the absolute value of the variable Ut, N defined by: Ut, N=$\sum_{i=1}^{1}\sum_{j=t+1}^{N} \boldsymbol{Dij}$

Where Dij = sgn (Xi-Xj) with sgn (X) = 1 if x > 0, 0 if x = 0 and -1 if x< 0

The Pettitt (1979) test was carried out in the Khronostat 1.01 software environment. In case the null hypothesis is rejected, an estimate of the break date is given by the time t, which defines the maximum in absolute value of the variable Ut, N.

In addition to identifying breaks, these climatological data were also used to calculate rainfall indices to assess the variation in rainfall from one year to the next. To do this, the reduced centred variable was used to highlight periods of surplus, deficit and normal rainfall (Dibi Kangah, 2010: 131; Bamba et al, 2020: 201). This method is expressed by the following formula:

$$l_i = \frac{X_i - \bar{X}}{\sigma}$$

with

l_i : Reduced centred index

X_i : Annual rainfall for the year i

$\bar{X}$: Average rainfall for the period 1971 - 2020

σ : the standard deviation of precipitation over the period 1971 - 2020

To better observe interannual variability, we used the method of reduced centred weighted moving averages or "Hanning's non-recursive low-pass filter of order 2, recommended by Tyson et al. (1975), cited by. N'da (2016: 85); Alamou et al, (2016: 318) and Adou et al (2020: 14). This method is effective because it allows the series to be visibly broken up, compensating for the shortcomings of the reduced centred index and the grouping of years by trend (Bamba et al, 2020: 201). In this case, the annual precipitation totals are weighted using the following equations (Fontaine et al, 1999):

X(t) = 0,06x(t-2) + 0,25 x(t-1) + 0,38 x(t) + 0,25 x(t+1) + 0,06 x(t+2)

For 3 ≤ t ≤ (n-2) where x(t) is the weighted precipitation total for term t. x(t-2) and x(t-1) are the precipitation totals for the two terms immediately preceding term t, and x(t+2) and x(t+1) are the precipitation totals for the two terms immediately following term t. The weighted precipitation totals for the first two [x(1), x(2)] and last two [x (n-1), x(n)] terms of the series are calculated using the following mathematical expressions (where n is the size of the series):

X*(1)* = 0,54x*(1)* + 0,46x*(2)*

X*(2)* = 0.25x*(1)* + 0.50x*(2)* + 0.25x*(3)*

X*(n-1)* = 0.25x*(n-2)* + 0.50x*(n-1)* + 0.25x*(n)*

X*(n)* = 0,54x*(n)* + 0,46x *(n-1)*

The results obtained are interpreted in three ways. If the value of the index is less than zero (< 0), there is a rainfall deficit for the year for which the index was calculated. If the value is greater than zero (> 0), there is a rainfall surplus. If the index is equal to zero (0), the rainfall is considered normal.

It should be noted that the Pettitt (1979) break detection test was chosen for its reliability and robustness. In the Pettitt (1979) test, the null hypothesis is the absence of a break in the series (Xi) of size N (Sultan and Janicot, 2004). The test assumes that for each time t between 1 and N, the time series (Xi) i=1 to t and t+1 to N belong to the same population. The variable to be tested is the maximum absolute value of the variable Ut, N, defined by the following mathematical formula:

$$U_{t,N} = \sum_{i=1}^{t} \sum_{J=t+1}^{N} D_{ij}$$

où $D_{ij} = sgn(X_i - X_j)$, avec $sgn(X) = 1$ si $X > 0$, 0 si $X = 0$ et -1 si $X < 0$

If the null hypothesis is rejected, an estimate of the break date is given by the time t, which defines the maximum absolute value of the variable Ut, N.

Rainfall intensity or climatic aggressiveness (R factor)

The R factor indicates the climatic aggressiveness caused by rainfall intensity. It has been determined from average rainfall using mathematical models that correlate R with average annual rainfall (P) (Nacishali Nteranya, 2021: 6). In his work on soil loss

in Adiopodoumé (Côte d'Ivoire), E. J. ROOSE concluded that rainfall alone does not explain extreme weather events (Roose, 1975, 1977). The relationships between rainfall and rainfall risk become highly significant only when maximum intensities are measured over more than 20 minutes for erosion and 10 minutes for runoff (Roose, 1975, 1977). For the West African zone, the author's observations made it possible to establish a theoretical relationship (R / P = 0.50) between the mean annual climatic aggressiveness index (R) and the mean annual rainfall (P). This relationship was used to derive the climatic aggressiveness parameter R using the following equation:

R = P * 0,5

The greater the intensity of the rainfall, the greater the risk of a precipitation disaster. The R factor is expressed in (MJ.mm/ha/h/year). It corresponds to the annual average of the sum of the products of the kinetic energy of rain by its intensity over 30 consecutive minutes (Sbai and Mouadili, 2021: 668; El Hage Hassan et al, 2018: 5).

Mapping rainfall vulnerability risk

The susceptibility to rainfall risk has been spatialised by integrating three indices: flooding, erodibility and landslides in the form of mudflows.

Flooding index

The flooding of a soil is equivalent to its topographical propensity to pond or drain vertically during excessive rainfall due to impermeability or limited drainage. This propensity was assessed using a topographic wetness index, specifically the SAGA Wetness Index (SAGAWI), based on the approach described Varin et al., (2017), Drolet (2020) and Traoré (2023). Empirically, SAGAWI values vary from a minimum of 0 for dry soils to a maximum of 25 or even 30 for wet soils (Varin, 2021: 5).

Erodibility index

The erodibility index was determined using the Universal Soil Loss Equation (USLE) of Wischmeier and Smith (1965) revised by Renard et al. (1997). RUSLE estimates the long-term average annual soil loss due to sheet and wind erosion (Panagos et al, 2015: 439). This equation includes five factors to explain water erosion, namely climate aggressiveness, soil erodibility, the topographic factor including slope and slope length, land use and anti-erosion practices. It is written as follows:

A (t/ha/year) = R * K * LS * C * P

Based on mathematical relationships (Table 2), the five parameters of the RUSLE model were determined and an erodibility index was calculated.

TABLE II. EQUATIONS FOR SOIL LOSS PARAMETERS

Factor	**Equations**	**Reference**
A (t/ha/year) : Soil loss per unit area per year	**A (t/ha/year) = R * K * LS * C * P**	Renard et al. (1997).
R: Rainfall index characterising climatic aggressiveness	**R = P * 0,5**	Roose (1977)
- K: Erodibility index related to the soil's resistance to sheet and gully erosion;	**K = fcsand * fcl-si * forgc * fhisand**	Williams (1995)
LS: Topographic index combining the effect of both the length L and the slope S of the slope.	**LS = [0.065 + 0.0456 (slope) + 0.006541 (slope)²] * (length of slope ÷ constant)NN**	Stone et Hilborn (2012) :
C: Soil cover index	$CrA = 0.1\left(\frac{-NDVI+1}{2}\right)$	Colman (2018) Durigon et al (2014).
P: Support practices index.	**P = 0.2+ 0.03× S**	Wener (1981)

Landslide index in the form of mudflows

Landslides are linked to the dynamics of waterlogged slopes (Traoré, 2022: 125). They depend on the morphology of the site and human use of the land, and are characterised by the descent of material in the form of mudflows (Baud et al., 2018. 177; Gooré et al., 2016: 111). The approach integrates several physical and anthropogenic factors whose combination in space and time contributes to the occurrence of the risk. These factors are slope value, rock strength, slope exposure, slope shape and curvature, wetness index and a land use index (Traoré, 2022: 135). All these factors were weighted and ranked according to Saaty's (1984: 226) Analytical Hierarchy Process as developed by (Traoré, 2022: 236). As the input data had different resolutions, we resampled them according to the raster with the lowest resolution, i.e. 10 m. This operation was carried out using the Resample tool in the ArcGIS interface by cubic interpolation of the pixels (R. Caloz et al., 1993: 21; A. Mama et al., 2013: 79).

The three indices of flooding, erodibility and landslide susceptibility were cross-referenced. The resulting distribution data were discretised in four steps (De Smith et al., 2021) and are based on the Natural Thresholds (Jenks) algorithm as described in Jenks and Caspall (1971). A map of susceptibility to risk occurrence in the ADA was generated.

III. RESULT

3.1. Significant variability in thermal and precipitation regimes in the ADA

Located in the intertropical zone, the ADA is characterised by a hot, humid climate. Between 1981 and 2020, temperatures remained above 20°C throughout the year (Fig. 2). Day and night temperature ranges vary insensitively by about 1°C. However, there is a tendency for the average temperature to rise steadily (Fig. 2). This confirms the global warming trend. Over a period of about forty years, the temperature has risen by about 0.40°C, or 0.1°C per year. If this trend continues, the average temperature will have risen by 1°C by 2080.

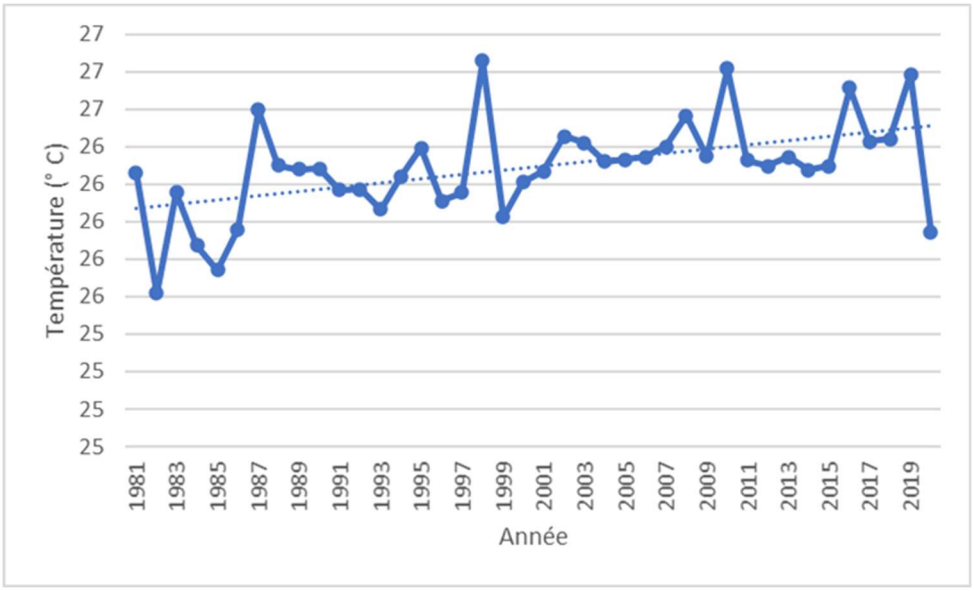

Fig. 2. Average annual temperature change between 1981 and 2020 (*Source: NASA, 2020 ; SODEXAM, 2017*)

3.2. Evidence of decline and significant inter-annual variability in rainfall

The ADA rainfall characteristics show that there was a significant break at the 90% threshold in 1982 (Fig. 3). Two sub-series stand out. One between 1971 and 1982 and the other between 1982 and 2020 (Table 3). The first sub-series (1971-1981) has an average rainfall of 1961.79 mm/year. The second period (1983-2020) records an average of 1629.33 mm/year. In contrast to the temperature, the cumulative precipitation for the period 1971-2020 shows a significant decrease, estimated at 332.46 mm/year, which represents a decrease of about 17% from the first to the second sub-series (Table 3).

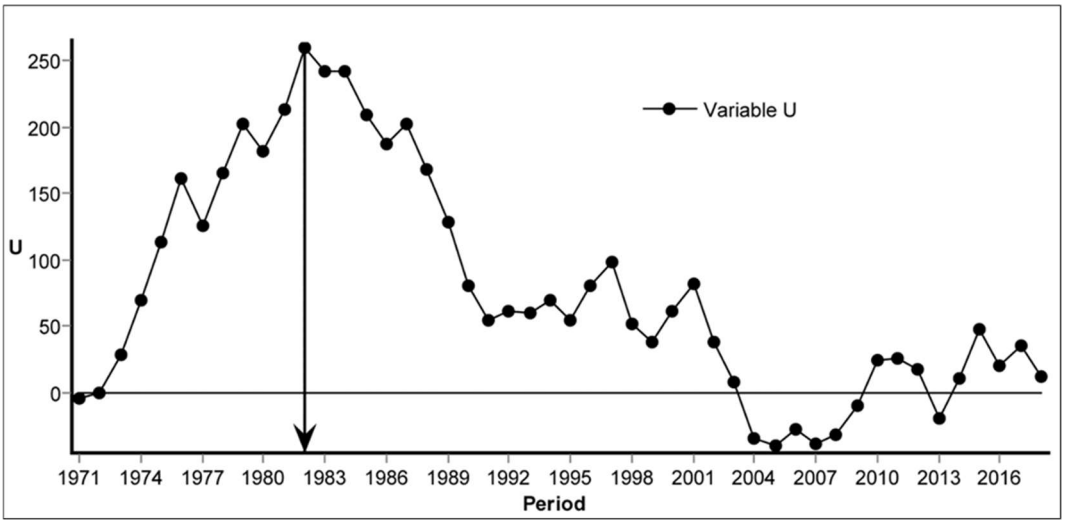

Fig. 3. Evolution of the variable U in the Pettitt tes (*Source: NASA, 2020 ; SODEXAM, 2017*)

TABLE III. BREAK IN STATIONARITY ACCORDING TO THE PETTITT TEST IN THE ADA RAINFALL SERIES

Location	Year of break	Average before break	Average after break	Standard deviation before break	Standard deviation after break	Regression rate
ADA	**1982**	**1961.79**	**1629.33**	**364.77**	**306.30**	**16.95% (332.46 mm)**

Source : NASA, 2020 ; SODEXAM, 2017

The first sub-series (1971-1981) has an average rainfall of 1961.79 mm/year. The second period (1983-2020) records an average of 1629.33 mm/year. In contrast to the temperature, the cumulative precipitation for the period 1971-2020 shows a significant decrease, estimated at 332.46 mm/year, which represents a decrease of about 17% from the first to the second sub-series (Table 3). However, the values of the standard deviations over the two sub-periods show a significant variation in rainfall around the averages from one year to the next. The calculation of rainfall indices has allowed us to assess the inter-annual variation in rainfall (fig. 4).

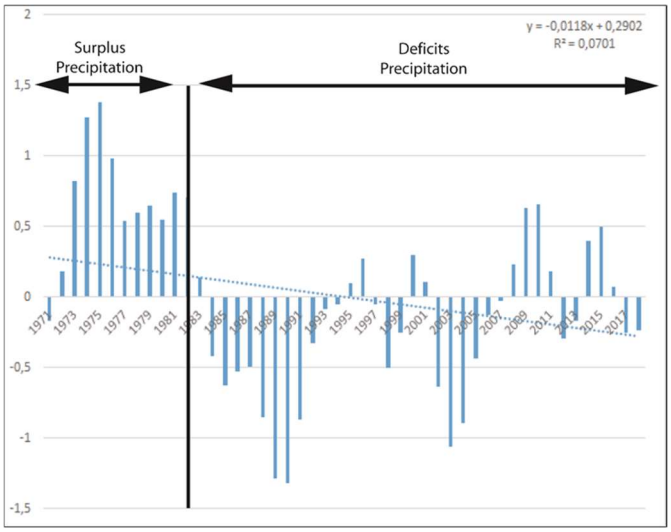

Fig. 4. Rainfall variability from 1971 to 2020 at the Abidjan station (*Source: NASA, 2020 ; SODEXAM, 2017*)

3.3. The R-factor for rainfall intensity or climatic aggressiveness

The breakpoint test of Pettitt (1974) and the calculation of rainfall indices make it possible to assess annual rainfall levels and variations. However, the relationships between rainfall and rainfall risk only become highly significant as rainfall intensities increase. The values of the R-factor vary between 704 and 751, with a mean of 723 and a standard deviation of 10.7 (Fig. 5).

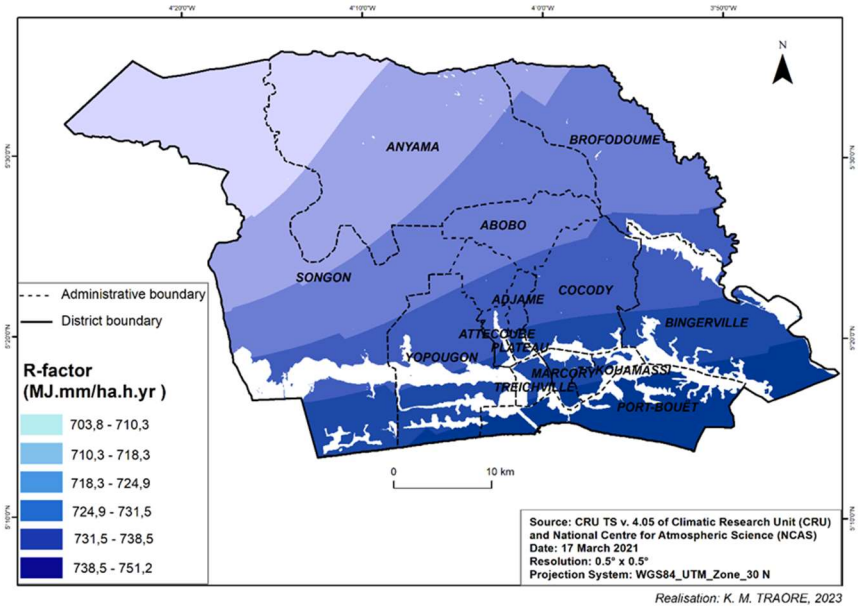

Fig. 5. R-factor for precipitation aggressiveness

This high rainfall intensity undoubtedly impedes vertical runoff from the ground and the removal of excess water by drainage systems, and is undoubtedly a risk factor for hydrometeorological disasters. A spatial analysis of this rainfall intensity (Fig. 4) shows that more than a third (36.7%) of the district is at a level between "fairly high" and "very high". This intensity increases from north-west to south-east (Fig. 4). The areas affected by this high intensity are mainly in the southern districts of Abidjan and almost a third of the communes of Bingerville, Cocody, Plateau and Yopougon (Fig. 5).

3.4. Susceptibility to rainfall risk in the ADA

The distribution values of the rainfall hazard range from a minimum (Xmin) of 3 to a maximum (Xmax) of 161. On analysis, the susceptibility to the occurrence of rainfall rik varies from 'very unlikely' to 'certain' (Fig. 6).

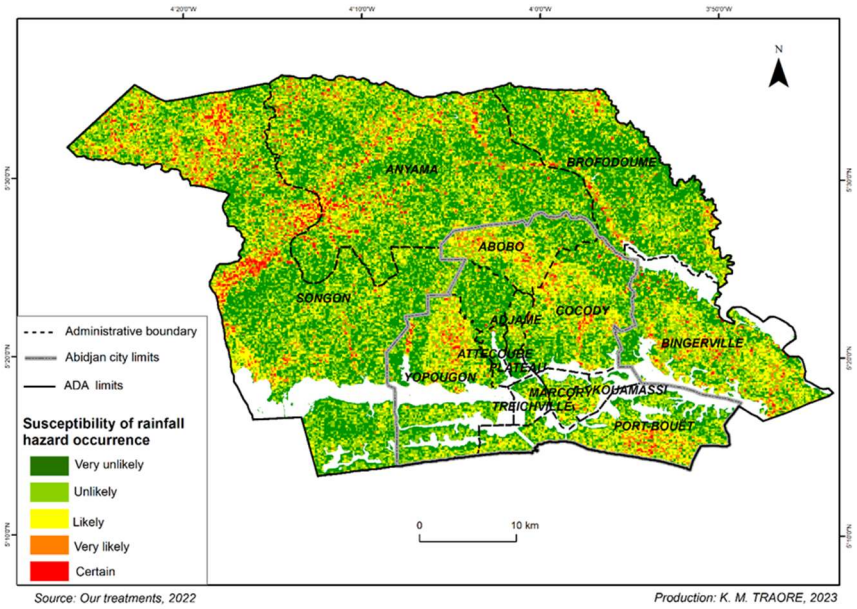

Fig. 6. Level of occurrence of rainfall risk in the ADA

Statically, the rainfall risk remains "Negligible" to "Marginal" over more than two thirds of the territory (table 2). The "Critical" and "Catastrophic" levels cover less than a tenth of the District (table 4).

TABLE IV. SPATIAL STATISTICS FOR RAINFALL RISK

N°	Susceptibility of rainfall hazard occurrence	Area (sq km)	Frequency (%)	Rainfall Risk
1	Very unlikely	646.9	35.3	Negligible
2	Unlikely	608.5	33.2	Marginal
3	Likely	426.6	23.3	Moderate
4	Very likely	111.5	6.1	Critical
5	Certain	37.9	2.1	Catastrophic

Source: Nos traitements, 2023.

However, this high rainfall risk affects the most densely populated communes, such as Yopougon, Abobo, Bingerville, Cocody and Port-Bouët. These communes are home to a total of 4.4 million people, or more than 7 out of 10 ADA inhabitants.

IV. Discussion

Extreme rainfall events are a major risk in the ADA. These findings are in good agreement with those of Hauhouot (2008: 80), Dongo et al. (2008: 8), Kangah and Alla Della (2015: 298), Kouassi and Alla Della (2021: 108). The main factor in these catastrophic events, which cause loss of life and major damage every year (Jah et al, 2015: 15), is the intensity of the rainfall (fig. 7), which varies from very heavy (up to 250 mm/h) in the first ten minutes to heavy (50 to 60 mm/h) after an hour (Hauhouot, 2008: 78). Not only will the intensity of these life-threatening weather phenomena increase, but their number and frequency will also increase with climate change (IPCC, 2023: 8).

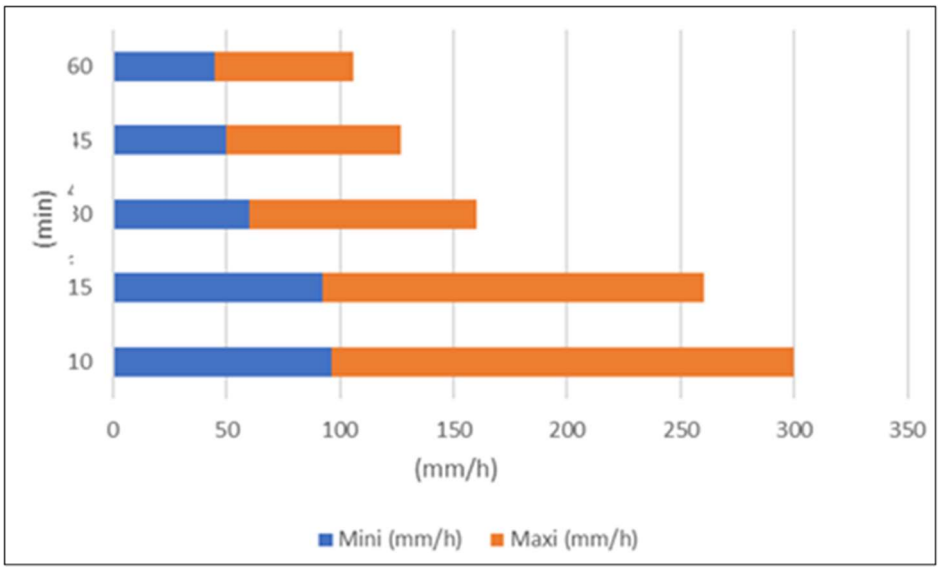

Fig. 7. Level of occurrence of rainfall risk in the ADA (*Source: NASA, 2020 ; SODEXAM, 2017*)

For example, "the heavy rains of June 21 were the strongest recorded since the beginning of the rainy season in the country, with nearly 200 mm of rain in less than 24 hours in several neighbourhoods of Abidjan and peri- urban areas" (IFRC, 2023: 1). Extreme hydro-meteorological events are intensifying and multiplying at an unprecedented rate around the world. The impressive 126 centimeters of rain that fell on the Hawaiian island of Kauai in 24 hours in April 2018 confirms this trend towards the intensification of hydro-meteorological events (IFRC, 2022: 23). Cyclical phenomena such as El Niño also contribute to this intensification of exceptional rainfall (Yeh et al, 2009; Cowan et al, 2023; Lee et al, 2023; Wang and Li, 2023; Koralegedara and al, 2023; Lal and Singh, 2023, Da Matta et al, 2023; Yu et al 2023).

In reality, apart from the intensification of rainfall hazards, other factors are also decisive in urban areas, such as rapid and anarchic urbanisation (Jah et al, 2012: 23; GCI, 2018: 34, Traoré, 2023: 15). Indeed, several studies have shown that, much more than climate change, it is the process of soil artificialisation induced by anarchic changes in land use and land cover that exacerbates the impact of extreme hydrometeorological events (Sbai and Mouadili, 2021; Simonneaux et al, 2015; Colman et al, 2019; Anache et al, 2018; Traoré, 2019; Traoré, 2023).

V. Conclusion

Overall, hydro-meteorological events are a major risk in the ADA. The resurgence of rainfall risk is due to disruptions in the elements of climate, manifested in the intensification and regularity of extreme weather events, but also to the vulnerabilities inherent in land use changes and poorly managed land tenure patterns. Climate change is merely a 'background factor' that exacerbates pre-existing territorial vulnerabilities. As the IFRC (2022: 27) reminds us, "climate change is a crisis - it is up to us to prevent it from becoming a disaster". The study is intended as a decision-making tool for local and national decision-makers, with a view to preventive management of climate crises.

VI. Acknowledgment

We would like to express our gratitude to the Programme d'Appui Stratégique à la Recherche Scientifique en Côte d'Ivoire (PASRES), the Fonds National pour la Science, la Technologie et l'Innovation (FONSTI) and the Centre Suisse de Recherche Scientifique (CSRS) for agreeing to finance the research of which a part of the results is presented in this article.

References

[1] ADO, J. P. et REY, J., 2020. Urbanisation et logement décents face aux risques météorologiques en Afrique : le cas d'Abidjan, Rapport, Centre for Affordable Housing Finance Africa, Abidjan, 12 p

[2] ADOU, A. G., N'DA, K. C., DAGNOGO, B. S. & KOLI B. Z., 2020. Variabilité pluviométrique et agriculture dans le bas-fond de Mahounou (Centre-ouest de la Côte d'Ivoire) DaloGéo, revue scientifique spécialisée en Géographie, 002 :. 12-27

[3] ALAMOU, E. A., QUENUM, G. M. L. D., LAWIN, E. A., BADOU, D. F., & AFOUDA, A. A., 2016. Variabilité spatio-temporelle de la pluviométrie dans le bassin de l'Ouémé, Bénin. Afrique Science, 12(3): 315-328.

[4] ANACHE, J. AA, FLANAGAN, D. C., SRIVASTAVA, A. and al., 2018. Land use and climate change impacts on runoff and soil erosion at the hillslope scale in the Brazilian Cerrado. Sci. Total Environ., 622–623 : 140–151,

[5] BAMBA, Y., KONÉ, M. et DIBI KANGAH, A. P., 2020. Variabilité pluviométrique et prévalence du paludisme à Grand-Bassam (Côte d'Ivoire). DaloGéo, revue scientifique spécialisée en Géographie, numéro spécial 001 : 12-27

[6] BAUD, P., BOURGEAT, S. & BRAS, C., 2018. Dictionnaire de géographie, Paris, Hartier, 607 p.

[7] BERTRAND, F., 2010. Changement climatique et adaptation des territoires. ZUINDEAU Bertrand. Développement durable et territoire, Presses universitaires du Septentrion, p. 339-350.

[8] BNETD, 2008, Atlas des villes : Abengourou, Abidjan, Bondoukou, Bouake, Daloa, Korhogo, Man, Odienne, San Pedro, Yamoussoukro, Côte d'Ivoire : Ministère d'état, Ministère du plan et du développement, 138 p.

[9] BROU, Y. T., 2008. La végétation du littoral ivoirien, Géographie du littoral de Côte d'Ivoire : éléments de réflexion pour une politique de gestion intégrée, La clonerie Saint-Nazaire, p 23-36.

[10] CALOZ, R., BLASER, T. J., & WILLEMIN, G., 1993. Création d'une ortho-image à l'aide d'un modèle numérique d'altitude : influences des modes de ré-échantillonnage radiométrique. aupelf-uref. Les Presses de l'université du Québec : 17-30.

[11] CAMIRAND J.et GINGRAS C., 2011. Les changements climatiques : quels en sont les causes et les impacts ? Nature Québec.

[12] COLMAN, C. B., OLIVEIRA, P. T. S., ALMAGRO, A., SOARES-FILHO, B. S., & RODRIGUES, D. B., 2019. Effects of climate and land-cover changes on soil erosion in Brazilian Pantanal. Sustainability, 11(24), 7053.

[13] COLOMBERT, M. et BOUDES, P., 2012. « Adaptation aux changements climatiques en milieu urbain et approche globale des trames vertes », VertigO Hors-série 12.

[14] COWAN, T., WHEELER, M. C., et MARSHALL, A. G., 2023. The combined influence of the Madden–Julian oscillation and El Niño–Southern Oscillation on Australian rainfall. Journal of Climate, 36(2): 313-334.

[15] DA MATTA, D. H., DOS SANTOS COELHO, C. A., DOS SANTOS, L. L., STONE, L. F., & HEINEMANN, A. B., 2023. Analysis of Goiás State rainfall and temperature similarity patterns during the El Niño-Southern Oscillation phenomenon phases across the years. Theoretical and Applied Climatology, 1-19.

[16] DE SMITH, M. J., GOODCHILD, M. F., & LONGLEY, P.., 2021. Geospatial Analysis- A Comprehensive Guide to Principles Techniques et Software Tolls 6th Edition.

[17] DIBI KANGAH, A. P., 2010. Rainfall and agriculture in Central West Africa since 1930 : Impact on Socioeconomic Development, LAP-LAMBERT Academic Publishing, Saarbrücken, 304 p.

[18] DONGO, K., CISSÉ, G. et BIÉMI J., 2008. Étude des inondations par débordement de réseau dans les milieux défavorisés d'Abidjan ; côte d'ivoire. In : Proceedings of the 13th IWRA World Water Congress, Global Changes and Water Resources, Montpelier, France. p. 1-4.

[19] DROLET, E., 2020. Identification des zones de contrainte de drainage aux opérations forestières à l'aide des données lidar, Mémoire, Université Laval, Québec, 62 p.

[20] EL HAGE HASSAN, H., CHARBEL, L., & TOUCHART, L., 2018. Modélisation de l'érosion hydrique à l'échelle du bassin versant du Mhaydssé. Békaa-Liban. VertigO, 18(1).

[21] EVANS, R., & BOARDMAN, J., 2016. The new assessment of soil loss by water erosion in Europe. Panagos P. et al., 2015 Environmental Science & Policy 54, 438–447—A response. Environmental Science & Policy, 58 : 11-15.

[22] FONTAINE, B., PHILIPPON, N., & CAMBERLIN, P., 1999. An improvement of June–September rainfall forecasting in the Sahel based upon region April–May moist static energy content (1968–1997). Geophysical Research Letters, 26(14) : 2041-2044.

[23] GCI (Gouvernement de Côte d'Ivoire), 2019. Evaluation des pertes, dommages et besoins suite aux inondations de juin 2018 à Abidjan, 2019, Programme ACP-UE de Prévention des Risques liés aux Catastrophes Naturelles, 220 p.

[24] GOORE F. J. B. L., TRAORE M.l, KOUASSI G. N., GOGBE T., 2016. Analyse spatiale des vulnérabilités et des risques de glissement de terrain a San-Pedro. ANYASÃ, Revue des Lettres et Sciences Humaines Laboratoire de Recherche sur la Dynamique des Milieux et des Sociétés, 6 :111-131.

[25] HAUHOUOT C., 2008. Analyse du risque pluvial dans les quartiers précaires d'Abidjan. Etude de cas à Attécoubé. Geo-Eco-Trop, 32 : 75-82.

[26] IFRC (International Federation of Red Cross and Red Crescent Societies), 2023. Côte d'Ivoire: Floods - DREF Operation Final Report, DREF operation no. MDRCI015, Operation n° FL-2022-000249-CIV, Informing humanitarians worldwide 24/7

[27] IFRC (International Federation of Red Cross and Red Crescent Societies), 2020. World Disasters Report 2020. Come Heat or High Water: Tackling the humanitarian impacts of the climate crisis together.

[28] IFRC (International Federation of Red Cross and Red Crescent Societies), 2020. Politique relative à la gestion des risques de catastrophe de la prévention à l'intervention et au relèvement, Genève, 8 p.

[29]

[30] INS (INSTITUT NATIONAL DE LA STATISTIQUE), 2008. Recueil des statistiques de l'environnement en Côte d'Ivoire. Abidjan, Institut national de la statistique, Département des statistiques et synthèses économiques.

[31] IPCC (Intergovernmental Panel on Climate Change), 2007. Climate change 2007: the IPCC fourth assessment Report, Summary for policymakers,

[32] IPCC (Intergovernmental Panel on Climate Change), 2014. Climate Change 2014 : Synthesis Report. Contribution of Working Groups I, II and III to the Fifth Assessment Report of the Intergovernmental Panel on Climate Change [Core Writing Team, R.K. Pachauri and L.A. Meyer (eds.)]. IPCC, Geneva, Switzerland, 151 p.

[33] IPCC (Intergovernmental Panel on Climate Change), 2022. Climate Change 2022: Impacts, Adaptation and Vulnerability.

[34] IPCC, 2022: Summary for Policymakers [H.-O. Pörtner, D.C. Roberts, E.S. Poloczanska, K. Mintenbeck, M. Tignor, A. Alegría, M. Craig, S. Langsdorf, S. Löschke, V. Möller, A. Okem (eds.)]. In: Climate Change 2022: Impacts, Adaptation and Vulnerability. Contribution of Working Group II to the Sixth Assessment Report of the Intergovernmental Panel on Climate Change [H.-O. Pörtner, D.C. Roberts, M. Tignor, E.S. Poloczanska, K. Mintenbeck, A. Alegría, M. Craig, S. Langsdorf, S. Löschke, V. Möller, A. Okem, B. Rama (eds.)]. Cambridge University Press, Cambridge, UK and New York, NY, USA, pp. 3–33,

[35] JENKS, G. F., & CASPALL, F. C., 1971. Error on choroplethic maps: definition, measurement, reduction. Annals of the Association of American Geographers, 61(2): 217-244.

[36] JHA A. K, BLOCH R. et LAMOND J., 2012. Villes et inondations, guide de gestion intégrée du risque d'inondation en zone urbaine pour le XXI siècle, résumé à l'intention des décideurs, Banque mondiale, Washington, 63 p.

[37] KANGAH, A. & DELLA ALLA André, 2015. Détermination des zones à risque d'inondation à partir du modèle numérique de terrain (MNT) et du système d'information géographique (SIG): Cas du bassin-versant de Bonoumin-Palmeraie (commune de Cocody, Côte d'ivoire). Geo-Eco-Trop, 39 (2) : 297-308.

[38] KOFFI, D. K., & DELLA, A. A., 2021. Catastrophes naturelles et vulnérabilités socio-économiques dans la commune de Cocody de 1990-2015. Espace Géographique et Société Marocaine, 1(52).

[39] KORALEGEDARA, S. B., HUANG, W. R., TUNG, P. H., & CHIANG, T. Y., 2023. El Niño-Southern Oscillation Modulation of Springtime Diurnal Rainfall Over a Tropical Indian Ocean Island. Earth and Space Science, 10(5), e2023EA002832.

[40] KOUNGBANANE, D., LEMOU F., DJANGBEDJA, M. & TOTIN, H. S. V., 2023. « Impacts socio-économiques et environnementaux des risques d'inondation dans le bassin versant de l'Oti au Togo (Afrique de l'Ouest) », VertigO - la revue électronique en sciences de

[41] LAL, D., & SINGH, S. (2023). Impact of El-Nino and La-Nina Episodes on Rainfall Variability and Crop Yield. International Journal of Environment and Climate Change, 13(10): 2046-2051.

[42] LEE, J. H., JULIEN, P. Y., CHO, J., LEE, S., KIM, J., & KANG, W., 2023. Rainfall erosivity variability over the United States associated with large-scale climate variations by El Niño/southern oscillation. Catena, 226, 107050.

[43] MAMA, A., SINSIN, B., DE CANNIERE, C., & BOGAERT, J., 2013. Anthropisation et dynamique des paysages en zone soudanienne au nord du Bénin. Tropicultura, 31(1).

[44] MANN, H. B., & WHITNEY, D. R.., 1947. On a test of whether one of two random variables is stochastically larger than the other. The annals of mathematical statistics : 50-60.

[45] MARTIN L., 1969. Introduction à l'étude géologique du plateau continental ivoirien : premiers résultats. Adiopodoumé : ORSTOM, 163 p. multigr. (Document Scientifique Provisoire - CRO ; 34).

[46] MARTIN, L., 1973. Carte sédimentologie du plateau continental de Côte d'Ivoire, Note explicative 48, Office de la Recherche Scientifique et Technique Outre-Mer, Paris, 25 p

[47] MCBEAN G. et AJIBADE I., 2009. Climate change, related hazards and human settlements. Current Opinion». Environmental Sustainability, 1 (2) : 179-186.

[48] N'DA, K. C., 2016. Variabilité hydroclimatique et mutations agricoles dans un hydrosystème anthropisé : l'exemple du bassin versant du Bandama en Côte d'Ivoire. Thèse de Doctorat unique en Géographie, Université Felix Houphouët Boigny, Abidjan, Côte d'Ivoire. 271 p.

[49] NACISHALI NTERANYA, J., 2021. Cartographie de l'érosion hydrique des sols et priorisation des mesures de conservation dans le territoire d'Uvira (République démocratique du Congo). VertigO-la revue électronique en sciences de l'environnement, 20(3).

[50] PETTITT, A. N., 1979. A non-parametric approach to the change-point problem». Journal of the Royal Statistical Society: Series C (Applied Statistics), 28 (2): 126-135.

[51] QUENAULT, B., 2013. Retour critique sur la mobilisation du concept de résilience en lien avec l'adaptation des systèmes urbains au changement climatique. EchoGéo, 24

[52] RENARD, K. G., FOSTER, G. R., WEESIES, G. A., MCCOOL, D. K., & YODER, D. C., 1996. Predicting soil erosion by water: A guide to conservation planning with the Revised Universal Soil Loss Equation (RUSLE). Agriculture handbook, 703, 400 p.

[53] ROOSE, E. J., 1977. Erosion et ruissellement en Afrique de l'Ouest, vingt années de mesures en petites parcelles expérimentales, travaux et documents de l'O.R.S.T.O.M n°78, Paris, 107 p.

[54] ROOSE, E., CHEROUX, M., HUMBEL, F.-X. (collab.), PERRAUD Alain (collab.)., 1966. Les sols du bassin sédimentaire de Côte d'Ivoire. Cahiers ORSTOM.Série Pédologie, 4 (2), p. 51-92.

[55] ROOSE, Eric J, 1975. Application de l'équation de prévision de l'érosion de Wischmeier et Smith en Afrique de l'Ouest," in communication au colloque sur la conservation et aménagement du sol dans les tropiques humides, Adiopodoumé, I.I.T.A. – Ibadan, 30/6 au 4/7/75 1 – 27.

[56] SAATY, T. L., 1984. The analytic hierarchy process: Decision making in complex environments. In : Quantitative assessment in arms control. Springer, Boston, MA: 285-308.

[57] SALACK, S., KLEIN, C., GIANNINI, A., SARR, B., WOROU, O.N., BELKO, N., BLIEFERNICHT, J., KUNSTMAN, H., 2016. Global warming induced hybrid rainy seasons in the Sahel, Environmental Research Letter, 11 (10) 11p.

[58] SBAI, A. & MOUADILI, O., 2021. Risque d'érosion hydrique entre fragilité des équilibres environnementaux et perspectives de durabilité : Cas du bassin d'Oued El Abed (Maroc nord-est). Revue Marocaine des Sciences Agronomiques et Vétérinaires, 9 (4) : 666-674.

[59] SIMONNEAUX, V., CHEGGOUR, A., DESCHAMPS, C. and al, 2015. Land use and climate change effects on soil erosion in a semi-arid mountainous watershed (High Atlas, Morocco). J. Arid Environ. 122, p. 64–75.

[60] STONE, R. P. and HILBORN, D.., 2012. Universal soil loss equation (USLE) factsheet. Ministry of Agriculture, Food and Rural Affairs, Ontario

[61] SULTAN, B., & JANICOT, S., 2004. La variabilité climatique en Afrique de l'Ouest aux échelles saisonnière et intra-saisonnière. I: mise en place de la mousson et variabilité intra-saisonnière de la convection. Science et changements planétaires/Sécheresse, 15(4) : 321-330.

[62] TRAORE K. M., 2022. Cartographie du risque de glissements de terrain en masse à l'échelle du District Autonome d'Abidjan (Côte d'Ivoire). RGO, Revue de Géographie de l'Université de OUAGA I Pr Joseph KI-ZERBO (BURKINA-FASO), 11, (3), p. 123-134

[63] TRAORE, K. M., 2023. Évaluation du risque d'inondation par intégration du SAGA Wetness Index (SAGAWI) et de l'Analyse Hiérarchique des Procédés (AHP): cas du District Autonome d'Abidjan ». Belgeo. Revue belge de géographie, 1, 29 p,

[64] TRAORE, K. M., 2023. Evaluation à l'aide du SAGA Wetness Index de l'inondabilité dans le District Autonome d'Abidjan, Côte d'Ivoire ». International Journal of Humanities and Social Science Invention (IJHSSI), 12 (4): 85-96.

[65] TRAORE, K. M., 2023. Monitoring of land use dynamics in the Autonomous District of Abidjan between 2002 and 2022 using the google earth engine platform. International Journal of Research and Review; 10(5): 255-268.

[66] TRAORE, K. M., YAO, K. E. et ADOU, A. G., 2019. Le fait urbain à l'épreuve des effets du réchauffement climatique : exemple de la crue du fleuve Bandaman à Bouaflé (Centre-ouest de la côte d'ivoire), Actes du colloque en hommage aux professeurs Bonaventure Maurice MENGHO et Marie-Joseph SAMBA KIMBATA, Baluki, 2019 (3ème année), n°5, Vol. III, p. 28-45.

[67] TYSON, P. D., DYER, T. GJ, et MAMETSE, M. N., 1975. Secular changes in South African rainfall: 1880 to 1972. Quarterly Journal of the Royal Meteorological Society, 101 (430): 817-833.

[68] UNOCHA (UN Office for the Coordination of Humanitarian Affairs), 2014. Côte d'Ivoire : Zones à risques d'inondations et de choléra (Juin 2014), Informing humanitarians worldwide 24/7

[69] VARIN, M., 2021. Analyse de l'efficacité de l'indice d'humidité topographique (TWI) à cartographier les milieux humides, Centre d'enseignement et de recherche en foresterie de SainteFoy inc. (CERFO). Rapport 2021-13. 28 p.

[70] WALLENHORST, N., ROBIN, J.-Y., & BOUTINET, J.-P., 2019. L'émergence de l'Anthropocène, une révélation étonnante de la condition humaine, p. 23-36

[71] WENER, C. G., 1981. Soil Conservation in Kenya, Ministry of Agri- culture, Soil Conservation Extension Unit, Nairobi, Kenya.

[72] WILLIAMS, J. R., & SINGH, V., 1995. The EPIC model. Computer models of watershed hydrology. Water Resour. Publ. Highl. Ranch Colo, 25: 909-1000.

[73] WISCHMEIER, W. H. et SMITH, D. D., 1965. Prediction rainfall erosion losses from cropland east of the Rocky Mountains: a guide for selection of practices for soil and water conservation. Washington, USDA. Agricultural Handbook 282: 47 p.

[74] YEH, S. W., KUG, J. S., DEWITTE, B., KWON, M. H., KIRTMAN, B. P., & JIN, F. F. 2009. El Niño in a changing climate. Nature, 461(7263): 511-514.

YU, S. Y., FAN, L., ZHENG, X. T., ZHANG, Y., ZHOU, Z. Q., & LI, Z., 2023. Sources of Inter-Model Diversity in the Strength of the Relationshi